JPE 9-6-8

Dynamic Coordination Strategies between HVDC and STATCOM

Chan-Ki Kim†, Vijay Sood*, and Seok-Jin Lee**

†KEPRI (Korea Electric Power Research Institute), Korea
*University of Ontario Institute of Technology (UOIT), Canada
**KEPCO (Korea Electric Power Corporation), Korea

ABSTRACT

This paper deals with the dynamic voltage control problem at the inverter end of a HVDC link when connected to a weak AC system which has the potential for harmonic instability and commutation failures. The dynamic voltage control problem is tackled with a STATCOM (Static Compensator), which not only provides a rapid recovery from harmonic instability and commutation failures but also offers a lower cost filter design for HVDC systems. PSCAD/EMTDC simulations are presented to validate the proposed topology and to demonstrate its robust performance.

Keywords: HVDC transmission, STATCOM

1. Introduction

Line commutated HVDC converters inherently consume large amounts of reactive power; typically, the reactive power demands of these converters are 50-60% of the DC power being transferred. For the design and safe operation of HVDC thyristor converters, there are special concerns when connecting to weak AC systems. These concerns include high temporary over voltages (TOVs), low frequency resonances, risk of voltage instability, harmonic instability, long fault recovery times and increased risk of commutation failure. Many of these concerns are closely related to AC voltage regulation at the converter bus. Some possible means of voltage regulation are the Synchronous Compensator (SC) (now virtually obsolete), the Static Var Compensator (SVC) and now the latest method, employing a Static Synchronous Compensator (STATCOM). The STATCOM option is likely to be employed with variable speed wind generator systems which will use voltage source converter (VSC) technology to connect to the grid.

Until now, HVDC systems and their associated reactive compensators were mostly operated and controlled independently. The interactions between HVDC system filters and reactive power compensator were largely considered under steady state conditions only. If the control between a HVDC system and its reactive power compensator can be actively coordinated, the performance of the HVDC will be improved in the transient state. This will also result in improved dynamic performance. With the industry increasingly leaning or being forced towards the integration of HVDC systems to weaker AC networks, the transient performance of such systems is of

Manuscript received Mar. 31, 2009; revised Sept. 23, 2009
†Corresponding Author: ckkim@kepri.re.kr
Tel: +82-42-865-5837, Fax: +82-42-865-5844, KEPRI
*University of Ontario Institute of Technology, Canada
** KEPCO (Korea Electric Power Corporation), Korea

vital importance. Earlier research [1] has indicated that the combination of SVCs with SCs provided much faster system response than SCs or SVCs alone. Other research [2] proposed a hybrid HVDC system coordinated with a STATCOM. A more modern topology, which considers the characteristics of the line-commutated HVDC with a STATCOM at the inverter end, is proposed in this paper. The proposed system consists of a black start function and a HVDC-STATCOM coordination control scheme. Furthermore, this paper investigates the advantages of the new STATCOM based system from the point of view of the cost reduction of the HVDC link filter design, recovery from commutation failures and overvoltage control as well as the dynamics of recovery from various system disturbances including undervoltage events. The main objectives of the proposed topology are (a) to dynamically control AC voltage at the inverter end of HVDC links, and (b) to achieve coordination control with HVDC systems.

The paper is structured as follows: first, the combined HVDC and STATCOM test system, along with the control strategies employed and the choice of the coordinating signal, are described in section 2: second, the impact studies of the STATCOM are presented in section 3: third, a number of dynamic simulation studies performed with a EMTDC/PSCAD are discussed. Finally, some concluding remarks are made.

2. HVDC- STATCOM System

2.1 Overall Test System

A diagram of the proposed HVDC-STATCOM system is shown in Fig. 1. The DC capacitor (Cdc) of the STATCOM is powered by an auxiliary supply consisting of a rectifier "B" that derives its energy from a diesel engine ("C"). The capacity of the system to provide reactive power support is determined by the STATCOM's MVA rating while its capacity to provide active power support depends mainly on the energy storage of the DC capacitor.

In Fig. 1, a diesel engine and a rectifier are used for the "black start" of the HVDC system which may be required to recover from a complete system shutdown. Before restarting the system, it will be necessary to disconnect the load from the HVDC inverter. The STATCOM is pre-charged to supply power to the HVDC system through the small diesel generator and a rectifier. The DC capacitor continues to be fed by the auxiliary power supply until the HVDC converter starts. When the DC capacitor is fully charged, the STATCOM output voltage is ramped up (giving smooth energization of the transformer) and then the HVDC converter can be de-blocked to commence transmitting active power. After the HVDC system has recovered, the disconnector switch is opened to isolate the auxiliary power supply from the DC capacitor of the STATCOM.

2.2 HVDC Test System

As shown in Fig. 1, the AC network parts of the HVDC study system and its DC controls are identical to those in the CIGRE benchmark model except for a STATCOM that is added to the AC bus bar at the inverter end.

The study system models a 1000 MW, 500 kV, 12 pulse, DC link with a low SCR receiving AC system. The STATCOM provides about 150 MVar at steady-state to fully compensate the inverter reactive power requirement. The simulations are conducted using the EMTDC transients simulation program.

With the STATCOM placed into the CIGRE benchmark model, the AC filter and fixed capacitor bank ratings have to be modified in order to maintain the reactive power demand of the inverter. Table 1 shows the parameters of the CIGRE model used in the simulation. For the purposes of this study, the STATCOM is modeled as a two-level Voltage Source Converter, switched at 1050 Hz, and rated at 150 Mvar.

Table 1. Parameters of CIGRE model.

Parameter	Rectifier	Inverter
SCR	2.5 angle-87degs	2.5 angle-75degs
ESCR	1.88 angle-86degs	1.9 angle-68degs
Bus Voltage(L-L)	345kV	230kV
Filter VAR supply	625 MVAr	620 MVAr
Nominal Angle	15degs	15degs

2.3 STATCOM Control (Fig. 2)

Fig. 2(a) shows the reactive power controller of an AC

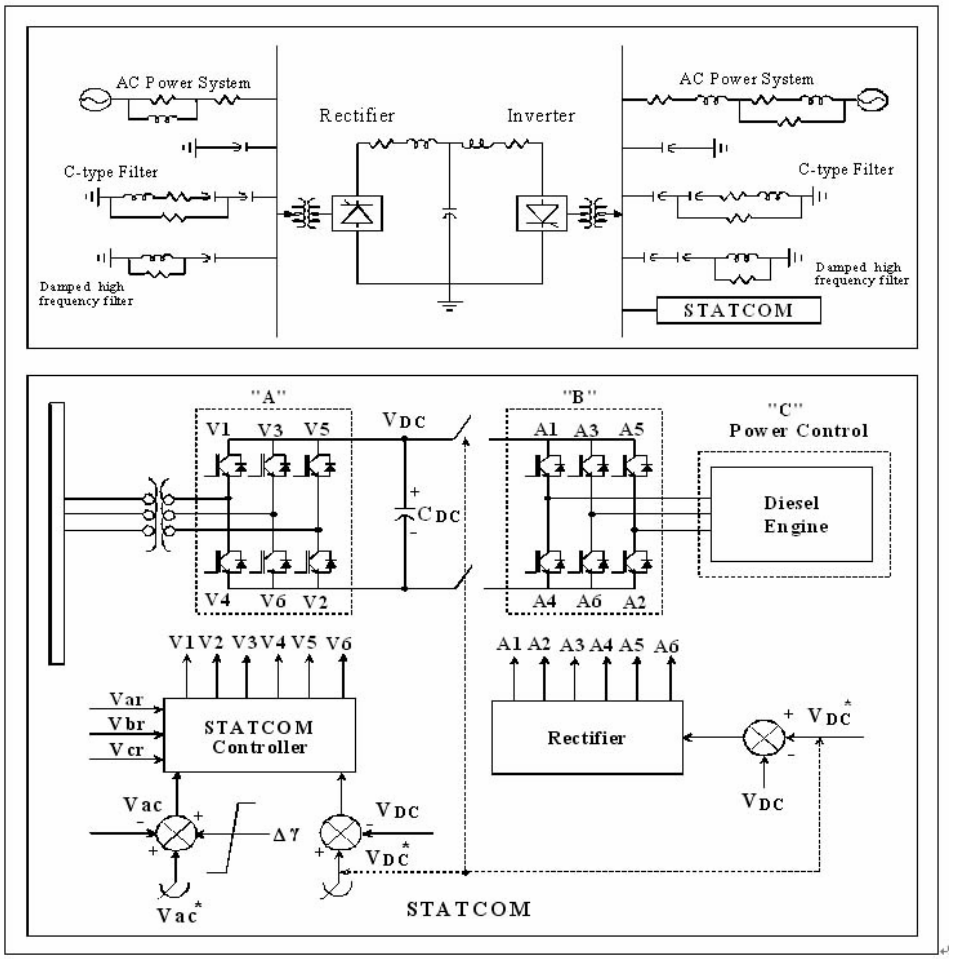

Fig. 1. Configuration of Proposed STATCOM System.

network. Fig. 2(b) shows the auxiliary control signal which modifies the control signal of the STATCOM based on the mean value of gamma (discussed later) at the inverter end of the HVDC system.

The AC voltage variations at the inverter bus of the HVDC system are directly related to the gamma value of the inverter. Hence, the gamma signal can be added to the voltage reference of the STATCOM to enhance system performance. In this way, it is possible to control the gamma to a specific range even during fast transients.

2.4 STATCOM Modeling

The terminal voltage and current of the STATCOM, at the point of connection, can be modeled by a vector representation. This vector representation is extended by a d-q model which leads to the definitions of instantaneous reactive current and active current. The voltage equations in the stationary a-b-c frame are:

$$e_a = L\cdot\frac{di_a}{dt} + V_a,\ e_b = L\cdot\frac{di_b}{dt} + V_b,\ e_c = L\cdot\frac{di_b}{dt} + V_c \quad (1)$$

Also, the voltage equations in the rotating d-q frame and the input voltages in the rotating d-q frame are shown in Equation (2).

$$e_d = L\cdot\frac{di_d}{dt} - \omega L i_d,\ e_q = L\cdot\frac{di_q}{dt} + \omega L i_d + V_q$$
$$e_d = |E|,\ e_d = 0 \quad (2)$$

Since the active power (P) supplied from the input is directly proportional to the d-axis current i_d, the d-axis reference current i'_d is generated from a proportional and

integral (PI)-type voltage controller for DC-link voltage regulation. Also the reactive power (Q) is directly proportional to the q-axis current i'_q, therefore, the reactive power equation and active power equation are shown in Equation (3).

$$P = \frac{3}{2} \cdot |E| \cdot i_d, \; Q = \frac{3}{2} \cdot |E| \cdot i_q \tag{3}$$

The voltage equations shown in Equation (1) are transformed from the stationary a-b-c frame to the rotating d-q frame as follows:

$$V_q = \omega L i_q + |E| + \Delta V_d, \; V_d = -\omega L i_d + \Delta V_q \tag{4}$$

Fig. 3 shows the STATCOM control block described in this section.

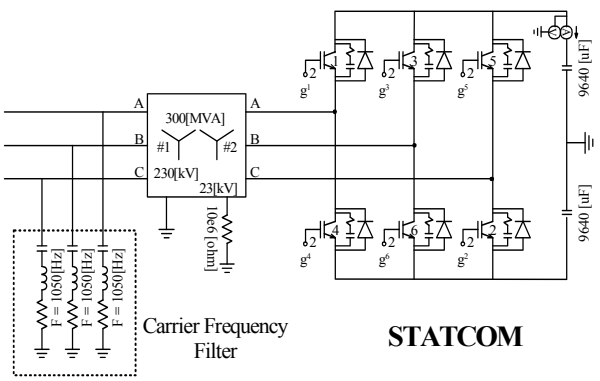

(a) STATCOM Converter

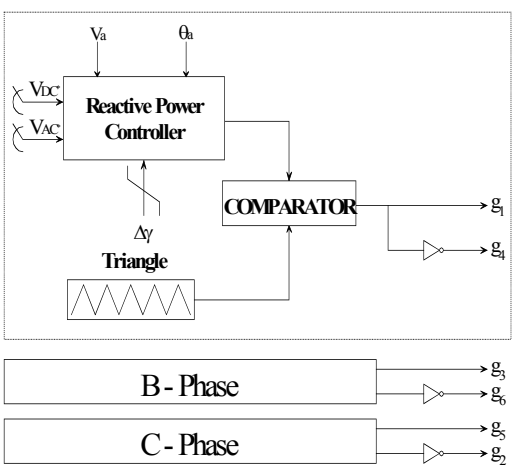

(b) STATCOM Controller

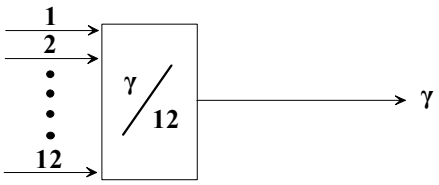

(c) Control Modifier using mean Gamma Signal

Fig. 2. STATCOM Control Function.

2.5 Selection of Auxiliary Signal in STATCOM

In HVDC control, as described in the well known CIGRE benchmark HVDC model [17], the primary control parameter on rectifier side is a DC current and the secondary control parameter is an alpha-minimum control. At the inverter side, the primary control parameter is a gamma-minimum control and the secondary control parameter is a DC current control.

In the case of installing a STATCOM on the inverter side of a HVDC system, a supplementary signal between the HVDC and the STATCOM must be considered in order to improve the coordinated performance between the HVDC and the STATCOM.

The following signals are candidates for suitable control coordination between a HVDC and a STATCOM: variations: in gamma ($\triangle \gamma$), DC current ($\triangle$I) and AC voltage ($\triangle V_{ac}$). Among these signals, $\triangle$I is not a good transient state control variable at the inverter end since DC current can oscillate at a fundamental frequency, and actually become sinusoidal during a prolonged commutation failure. However, on the rectifier side, a DC current signal could be a good control variable. Also, AC voltage as a coordinated supplementary signal can be considered, but because this signal is directly proportional to AC voltage and reactive power, its use as a control signal in the case of a STATCOM is not preferred.

The trajectory of a $\triangle \gamma$ value between active power (P_{dc}) and reactive power (Q_{dc}) in a HVDC system moves according to a cosine function (Fig. 4). If the gamma signal of a HVDC is added to the controller of a STATCOM, the gamma signal can be a useful signal for improving the performance of a STATCOM in a transient state.

However, there are two options for employing the gamma signal: either a mean value gamma γ_{mean} signal

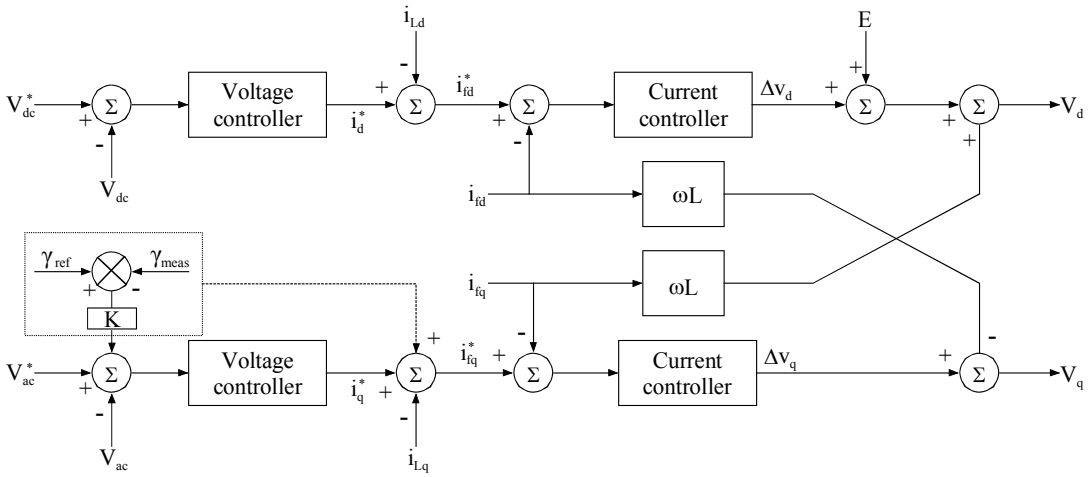

Fig. 3. STATCOM Controller Model.

or a minimum value gamma γ_{min} signal. The γ_{min} signal is more relevant for improving performance against a commutation failure, but the response time is inherently slower (when compared to the derivation of the γ_{mean}) due to the computation algorithm. On the other hand, the γ_{mean} is less relevant against commutation failure, but the response time is fast. Furthermore, the γ_{mean} is always higher than the γ_{min} value. This comparison is shown in Fig. 5(a) for the recovery of the system following a 3-phase fault at the inverter. Fig. 5(b) shows the recovery of the 3-phase AC voltages, and Fig. 5(c) shows the recovery of the corresponding DC current I_{dc} and DC voltage V_{dc}.

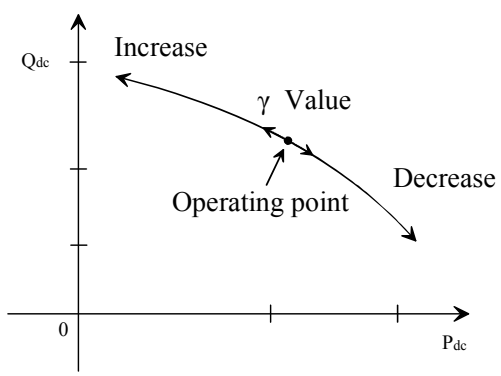

Fig. 4. Trajectory between active power and reactive power in HVDC.

Due to the relative speed of the response characteristics, a mean signal is selected as the coordinated supplementary signal of the STATCOM. The supplementary signal of the STATCOM is as follows:

$$\Delta\gamma = K[\gamma_{ref.} - \gamma_{meas.}] \quad (5)$$

A signal which represents gamma variation, as shown in Equation (5), is added to the STATCOM controller.

3. Impact of the STATCOM

The impact of the STATCOM is felt upon the following system aspects:

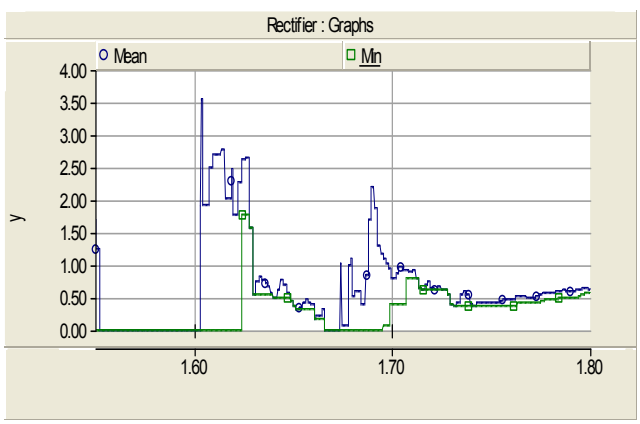

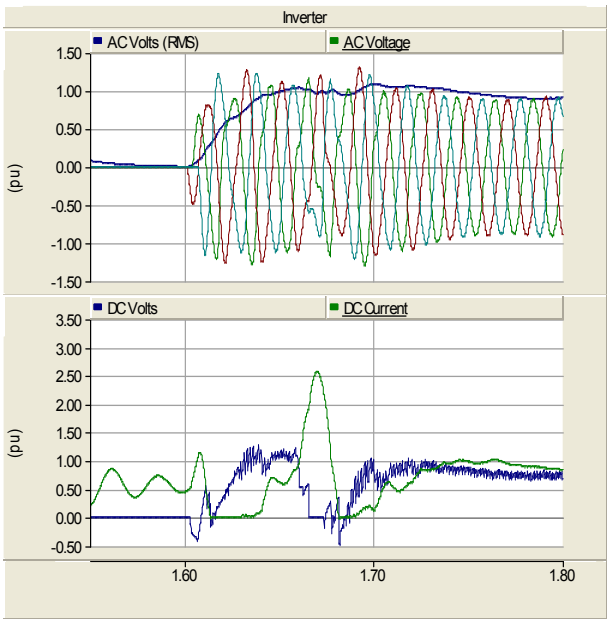

Fig. 5. Recovery for 3-phase AC Fault at inverter. (a) Comparison of mean value of gamma vs. minimum value of gamma, (b) Recovery of 3-phase voltages at inverter, (c) DC voltage and DC current.

3.1 Counter-acting Commutation Failures (CFs)

Commutation failure (CF) is one of the most frequent inverter failures in HVDC systems utilizing thyristor valves. Before the valve can establish a forward voltage blocking capability, the internal stored charges in the valve, produced during the forward conduction interval, must be removed. Therefore, the valve requires a certain minimum negative voltage-time area, provided by the commutation margin angle, to re-establish its blocking capability. Otherwise, the valve will immediately re-conduct when it is again forward biased and that will result in an unwanted short-circuit and a CF may ensue.

CFs can be detrimental to HVDC links. For instance, they can result in a significant direct current increase and thus lead to overheating of the converter valves which will shorten their lifespan. In addition, CFs can cause DC magnetic biasing in the converter transformers, and may even lead to an outage of the HVDC system. From this perspective, CFs can be considered as an index of the non-availability of the HVDC link.

A CF is a very complex phenomenon to analyze. Reference[9] proposed an empirical equation for defining CFs, as shown in Equations (6) and (7). In these equations, the possibility of a CF is expressed by $\triangle V$ which is the onset voltage of a CF. Equation (6) is for a 3-phase fault case and Equation (7) is for a 1-phase fault case:

$$\Delta V = 1 - \frac{i'_d}{i_d} \bullet \frac{X_{cpu}}{X_{cpu} + \cos\gamma_0 - \cos\gamma} \tag{6}$$

$$\Delta V = 1 - \frac{i'_d}{i_d} \bullet \frac{X_{cpu}}{X_{cpu} + \cos(\gamma_0 + \theta) - \cos\gamma} \tag{7}$$

where, i'_d is a larger DC current, X_{cpu} is the impedance of the converter transformer, γ_0 is the thyristor extinction angle, γ is the thyristor operation angle and θ is the AC voltages intersection deviation angle due to a 1-phase fault. From Equation (6) and (7), a larger DC current (i'_d) can be re-arranged as shown in Equation (8):

$$i'_d = L_T \bullet \frac{dv}{dt} \tag{8}$$

where, $L_T = 2 \cdot L_{smoothing} + L_{Line} + X_{cpu,}$ $dv = V_{Postfault} - V_{postfault}$ dt is the fault clearing time, $V_{postfault}$ is the AC voltage after a fault and $V_{postfault}$ is the AC voltage before a fault. $L_{Smoothing}$ is an inductance of the smoothing reactor and L_{Line} is an inductance of a cable or overhead line.

Equations (6) and (7) show that the primary reasons for CFs are current increases and extinction angle deviations of the HVDC converter due to AC voltage reductions which can be caused by:

- AC voltage faults/disturbances
- Transformer inrush current
- Capacitor inrush current
- Harmonic pollution or/and instability
- System induced resonances

From the above explanations, the obvious solution to reduce the risk of CFs is to maintain a constant margin

angle and a constant AC voltage. From Equation (7), the conditions and equations for critical load variations (transformer energizing and capacitor switching etc.) to induce CFs can be shown as Equation (9):

$$\left(1-\frac{i'_d}{i_d}\cdot\frac{X_{cpu}}{X_{cpu}+\cos\gamma_0-\cos\gamma}\right)\times SCR > Tr_{.scc-pu} \qquad (9)$$

where, $Tr_{.scc-pu}$ is the short circuit capacity a of transformer to connect to a AC bus bar.

In this paper, several cases are simulated to show the impact of a STATCOM. The simulation conditions are as follows: SCR=2.5 based on the CIGRE benchmark model, the capacity of the STATCOM is 150 MVA and the operational set point condition is 0 MVAR (i.e. it is "floating"). Also the simulation cases are with transformer energization and remote faults according to distance from the fault.

Tables 2 to 4 show the occurrence of CFs according to transformer energization. The STATCOM operating point is varied from 0 MVA for Table 2, lagging 50 MVA for Table 3, and leading 50 MVA for Table 4.

Table 2. CFS(Commutation Failures) According to Transformer Energization (STATCOM: 0 MVA).

Capacity MVA	**CFs** (With STATCOM)	**CFs** (Without STATCOM)
300	No-CFs	No-CFs
400	No-CFs	CFs
500	CFs	CFs
600	CFs	CFs

Table 3. CFs According to Transformer Energization (STATCOM : Lagging 50 MVA).

Capacity MVA	**CFs** (With STATCOM)	**CFs** (Without STATCOM)
300	No-CFs	No-CFs
400	No-CFs	CFs
500	No-CFs	CFs
600	CFs	CFs

From Tables 2, 3 and 4, it can be seen that as the Capacity MVA is increased from 300 to 600 MVA, CFs appear earlier without the STATCOM i.e. at the 400 MVA level. Although it is difficult to quantify the actual significance of the STATCOM in reducing the occurrence of CFs, the beneficial trends are obvious from these tables.

Table 4. CFs According to Transformer Energization (STATCOM: Leading 50 MVA).

Capacity MVA	**CFs** (With STATCOM)	**CFs** (Without STATCOM)
100	CFs	CFs
200	No-CFs	No-CFs
300	No-CFs	No-CFs
500	No-CFs	No-CFs

Table 5 shows the result in the case of a remote fault according to its distance from the commutating bus. The STATCOM is held in neutral mode (i.e. 0 MVA supply) for this case. With the STATCOM present, CFs are experienced at distances of 200 km or less. However, without the STATCOM, these distances are extended to 300 km or less. The beneficial impact of the STATCOM is evident.

Tables 6 and 7 are cases with and without the complementary control in a STATCOM in operation. From Table 6, with the complementary control in a STATCOM, CFs are experienced after the 500 MVA capability of the transformer energization. However, without the complementary control in a STATCOM, CFs are experienced at less than 450 MVA. Again the beneficial impact of the STATCOM is evident.

Table 5. CFs According to Distance (Remote Faults) (STATCOM: 0 MVA).

Distance km	**CFs** (With STATCOM)	**CFs** (Without STATCOM)
100	CFs	CFs
200	CFs	CFs
300	No-CFs	CFs
500	No-CFs	No-CFs

Table 6. CFs According to Transformer Energization (STATCOM: 0 MVA).

Capability MVA	**CFs** (With Complementary Control in STATCOM)	**CFs** (Without Complementary Control in STATCOM)
400	No-CFs	No-CFs
450	No-CFs	CFs
500	CFs	CFs

As shown in Table 7, the incidences of CFs in relation to the distance to a remote fault are investigated. With the STATCOM complementary control in operation, the distance to a fault can be extended beyond 250 kms without causing CFs. However, without the STATCOM, this distance has to be increased to beyond 250 kms. Again the benefits of the STATCOM are evident.

Table 7. CFs According to Distance (Remote Faults) (STATCOM: 0 MVA).

Distance km	**CFs** (With Complementary Control in STATCOM)	**CFs** (Without Complementary Control in STATCOM)
200	CFs	CFs
250	No-CFs	CFs
300	No-CFs	No-CFs

3.2 Complementing HVDC Filter Unit Size

Typically, the filter bank size in a HVDC system is determined to obtain a net voltage step of 5% under the minimum short circuit level condition. However, if the voltage step can be controlled, the filter unit size can be larger and, consequently, the number of filter banks can be reduced. Such characteristics can also reduced the amount of filter switching and enhance system reliability.

3.3 Robustness against Harmonic Pollution

From Equations (6) and (7), the main causes of CFs are DC over-currents and AC voltage reduction. AC harmonics are another major factor which can cause CFs in HVDC converters. Fig. 6 conceptually shows how the extinction angle is reduced due to the 3rd and 5th harmonic components in AC voltage. A STATCOM is the designated component to supply reactive power to an AC network. Functionally this is done in the same manner as a synchronous condenser or a SVC, and structurally, it is done in a similar manner to an active power filter or power conditioner. Fortunately, because a STATCOM is composed of self-commutating semiconductors, it has an inherent immunity to externally generated harmonics.

Table 8 shows the reduced harmonic spectrums and the filtering capability against harmonics, in the cases that the harmonics (2nd, 3rd, 5th and 7th harmonics) are arbitrarily injected into a CIGRE model with and without a STATCOM. In Table 8, the 2nd harmonic is reduced to 60%. This result shows that a STATCOM can contribute to stability enhancement by reducing the 2nd harmonic resonance condition which causes core saturation instability.

Table 8. Harmonic Mitigation due to STATCOM (Condition: Injected Harmonic Current: 1000A, Injected Harmonics: 2nd, 3rd, 5th and 7th, Measured Point: AC Bus Terminal, Target AC Network: Pure AC Network without Filters (for Example: 11th, 13th Filters for HVDC).

Harmonics	**With STATCOM**	**Without STATCOM**	**Difference %**
2nd Harmonic	238	323	73.6%
3rdHarmonic	245	333	73.5%
5thHarmonic	269	323	83.3%
7th Harmonic	294	322	91.3%

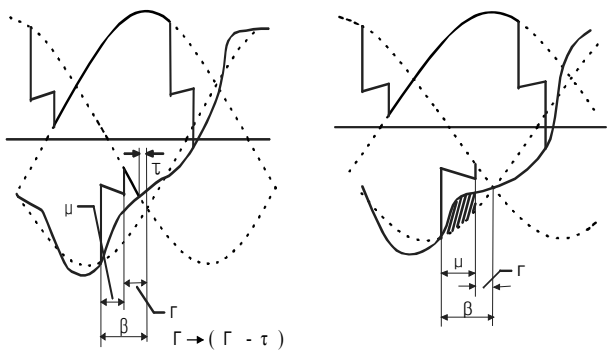

Fig. 6. Extinction angle reduction due to harmonic.

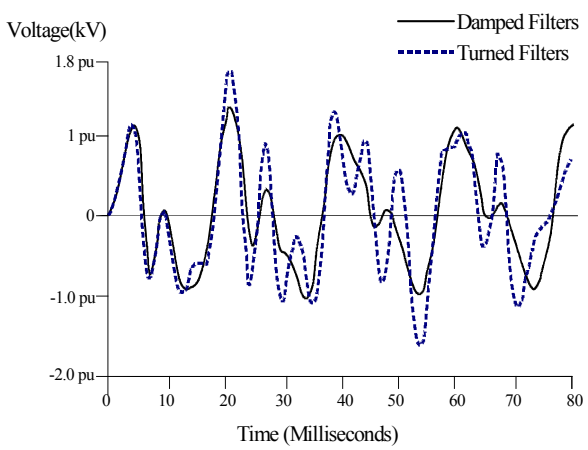

Fig. 7. Fault recovery characteristics of AC network with tuned and damped filters.

Two kinds of filters are normally used in HVDC systems, i.e. tuned and damped filters. Tuned filters are used for suppressing only characteristic harmonics. On the other hand, damped filters are often employed for the suppression of both non-characteristic and characteristic harmonics. The capital cost of tuned filters is lower than for damped filters, despite the fact that a separate filter bank is required for each of the lower-order characteristic harmonics. This cost advantage is one of the reasons for the use of tuned filters.

However, an AC system has numerous other harmonic sources apart from the DC link. AC harmonic filters play a major role in determining the waveform quality and amplitude of the switching surge overvoltages on the converter bus bar. In HVDC systems, transients should be considered as an integral part of the filter design for harmonic suppression. The effect on both the converter station and the existing AC system should be evaluated as part of the overall design process. Fig. 7 shows the fault recovery characteristics of the CIGRE HVDC model with either damped filters or tuned filters. The fault investigated is the recovery from a 3-phase to ground fault, which usually produces the highest overvoltages and harmonics, with the converters blocked. From Fig. 7, an AC network including a HVDC with damped filters can have recovery characteristics after a fault that are as good as a network with tuned filters. Despite the capital disadvantages, this characteristic is one of the reasons for the widespread use of tuned filters.

Consequently, if a STATCOM is connected to a HVDC terminal, an AC network with tuned filters can have good recovery characteristics after a fault.

4. HVDC-STATCOM Simulations

4.1 Case Studies

Comparative studies of two system configurations of the CIGRE model (one with a STATCOM and the other without a STATCOM) were preformed. In these cases, the consideration was the converter transformer energization and its resulting saturation, which causes voltage and current distortion and repeated commutation failures at the inverter end. The results with two fault cases (either 1-phase or 3-phase faults at the inverter bus) are presented below.

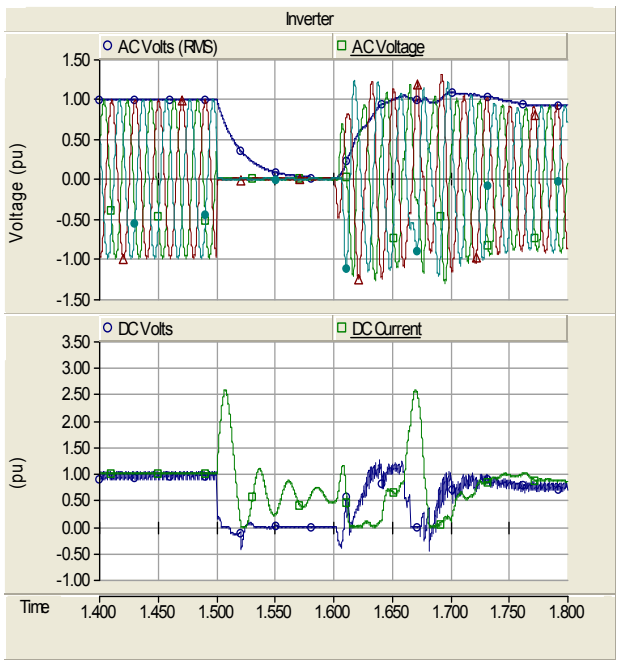

(a)

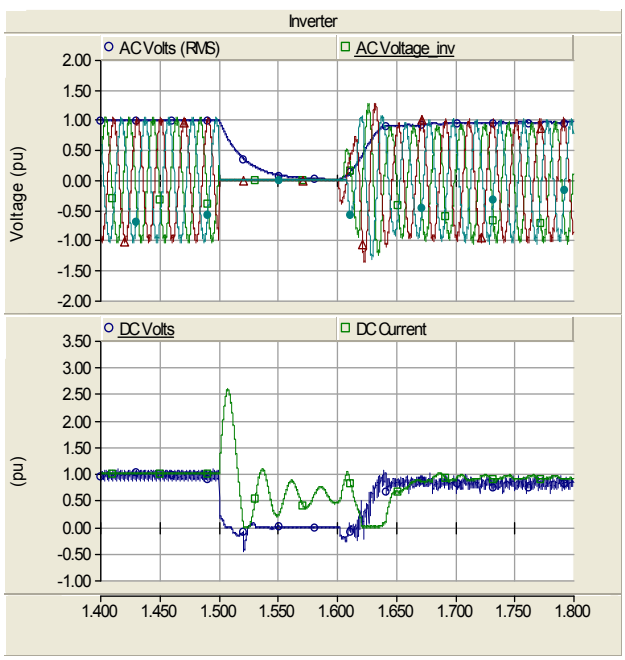

(b)

Fig. 8. Response of the HVDC system in the case of considering the Saturation Characteristics of Transformer. (At 3-phase grounded fault).

4.2 Results

Fig. 8(a) shows the case of a 3-phase fault at the inverter end on the CIGRE Model without a STATCOM. During the recovery of the HVDC system, repeated commutation failures were seen. This should be compared with Fig. 8b where a corresponding case with a STATCOM in place is depicted. The results show that the repeated commutation failures were not observed. In this case, the impact of the STATCOM on the recovery of the system is quite conclusive.

5. Conclusions

This paper deals with the use of a STATCOM at the inverter end of a conventional HVDC system for dynamic reactive power support. This new topology has a number of benefits. First, with the aid of an auxiliary source, this topology permits a black start feature. The proposed scheme may be a good solution for connecting island loads, offshore oil platforms or offshore wind farms. The proposed solution can be used with both cables and overhead lines. Second, with the reactive power coordination between STATCOM and HVDC systems, it offers robustness in recovery from commutation failures, and other faults in the system. Third, with the ability of the STATCOM to act as an active filter, the design of the passive filters of the HVDC system can be eased somewhat; this will enable recouping some of the costs incurred in the installation of a STACOM. In this paper, the coordinated control strategy for a STATCOM-HVDC has been described.

References

[1] Nayak, O.B.; Gole, A.M.; Chapman, D.G.; Davies, J.B.;, "Dynamic performance of static and synchronous compensators at an HVDC inverter bus in a very weak AC system," *IEEE Transactions on Power Systems*, Vol. 9, Issue 3, pp. 1350-1358, Aug. 1994.

[2] Andersen, B.R.; Lie Xu;, "Hybrid HVDC system for power transmission to island networks," *IEEE Transactions on Power Delivery*, Vol. 19, Issue 4, pp. 1884-1890, Oct. 2004.

[3] Faruque, M.O.; Yuyan Zhang; Dinavahi, V.;, "Detailed modeling of CIGRE HVDC benchmark system using PSCAD/EMTDC and PSB/SIMULINK," *IEEE Transactions on Power Delivery*, Vol. 21, Issue 1, pp. 378-387, Jan. 2006.

[4] Kuang Li; Jinjun Liu; Zhaoan Wang; Biao Wei;, "Strategies and Operating Point Optimization of STATCOM Control for Voltage Unbalance Mitigation in Three-Phase Three-Wire Systems," *IEEE Transactions on Power Delivery*, Vol. 22, Issue 1, pp. 413-422, Jan. 2007.

[5] Jain, A.; Joshi, K.; Behal, A.; Mohan, N.;, "Voltage regulation with STATCOMs: modeling, control and results," *IEEE Transactions on Power Delivery*, Vol. 21, Issue 2, pp. 726-735, April 2006.

[6] Garica-Gonzalez, P.; Garcia-Cerrada, A.;, "Control system for a PWM-based STATCOM," *IEEE Transactions on Power Delivery,* Vol. 15, Issue 4, pp. 1252-1257, Oct. 2000.

[7] Shen, D.; Lehn, P. W.;, "Modeling Analysis and Control of a Current Source Inverter-Based STATCOM," *IEEE Power Engineering Review*, Vol. 21, Issue 11, pp. 61-61, Nov. 2001.

[8] Hanson, D.J.; Woodhouse, M.L.; Horwill, C.; Monkhouse, D.R.; Osborne, M.M.;, "STATCOM: a new era of reactive compensation," *Power Engineering Journal*, Vol. 16, Issue 3, pp. 151-160, June 2002.

[9] Thio, C.V.; Davies, J.B.; Kent, K.L.;, "Commutation failures in HVDC transmission systems," *IEEE Transactions on Power Delivery,* Vol. 11, Issue 2, pp. 946-957, April 1996.

[10] Kristmundsson, G.M.; Carroll, D.P., "The effect of AC system frequency spectrum on commutation failure in HVDC inverters," *IEEE Transactions on Power Delivery*, Vol. 5, Issue 2, pp. 1121-1128, April 1990.

[11] Galanos, G., Vovos, N., Giannakopoulos, G., "Combined control and protection system for improved performance of HVDC links in the presence of AC faults," *IEE Proceedings Generation, Transmission and Distribution*, Vol. 131, Issue 4, pp. 129-139, July 1984.

[12] Working Group 14.02, "Commutation failures in HVDC transmission systems due to AC system faults," *Electra,* Vol. 169, No. 1, pp. 59-85, Dec. 1996.

[13] L. Zhang and L. Dofnas, "A novel method to mitigate commutation failure in HVDC systems," *in Proc. IEEE Power System Technology Conf.*, Vol. 1, pp. 51-56, Oct. 2002.

[14] A. Hansen and H. Havemann, "Decreasing the commutation failure frequency in HVDC transmission systems," *IEEE Trans. on Power Del.*, Vol. 15, No. 3, pp. 1022-1026, Jul. 2000.

[15] S. Tamai et al., "Fast and predictive HVDC extinction angle Control," *IEEE Trans. on Power Systems*, Vol. 12, No. 3, pp. 1268-1275, Aug. 1997.

[16] M. sato, K. Yamaji, and M. Sekita, "Development of a hybrid margin angle controller for HVDC continuous operation," *IEEE Trans. on Power Systems*, Vol. 11, No. 4, pp. 1792-1798, Nov. 1996.

[17] M. Szechtman, T. Wess, and C. V. Thio, "First benchmark Model for HVDC control studied," *Electra*, Vol. 135, No. 4, pp. 54-73, 1991.
[18] S. Nyati, S.R. Atmuri, et al., "Comparison of Voltage Control Devices at HVDC Converter Stations Connected to Weak AC Systems," *IEEE Transactions on Power Delivery*, Vol. 3, No. 2, pp. 684-693, April 1998.

Chan-Ki Kim obtained his M.S and his Ph.D. in Electrical Engineering from Chung-Ang University, Korea, in 1993 and 1996 respectively. Since 1996, he has been with KEPRI, the R&D center of KEPCO (Korea Electric Power Corporation). His research interests are HVDC, Power Electronics and Generator Control. He received a Technical Award from the Ministry of Science & Technology, Korea and Excellent Paper Awards from KIEE in 2002 and 2004 respectively. Currently, he is working at KEPRI. He is a Senior Member of the Institute of Electrical and Electronics Engineers (IEEE).

Vijay Sood obtained his B.Sc. (1st Class Hons.) from University College, Nairobi and his M.Sc. from Strathclyde University, Glasgow in 1969. He obtained his Ph.D. in Power Electronics from the University of Bradford, England in 1977. From 1969 to 1976, he was employed at the Railway Technical Centre, Derby. From 1976 to 2006, he was employed as a Researcher at IREQ (Hydro-Québec) in Montreal. Presently, he is on special assignment at the University of Ontario Institute of Technology (UOIT) in Oshawa, Ontario. He is a Fellow of the IEEE and a member of the IEE (UK). He is also the Editor of the IEEE Transactions on Power Delivery, Co-Editor of the CJECE and an Associate Editor of the Journal Control Engineering Practice.

Seok-Jin Lee obtained his B.S. and M.S. in Electrical Engineering from Seoul National University, Seoul, Korea, in 1980 and 1982, respectively. He was the designer of Cheju HVDC #1 in 1992 and the manager of Cheju HVDC #1 in 1994. His is interested in HVDC and Power Quality. He received a First National Electrical Engineer License from the Korea Government in 1983. He is the author or co-author of more than 30 technical publications and he has 5 patents related to HVDC. At present, he is a vice-director in KEPCO (Korea Electric Power Corporation).